

We are IntechOpen, the world's leading publisher of Open Access books Built by scientists, for scientists

6,900

Open access books available

186,000

International authors and editors

200M

Downloads

Our authors are among the

154

Countries delivered to

TOP 1%

most cited scientists

12.2%

Contributors from top 500 universities



WEB OF SCIENCE™

Selection of our books indexed in the Book Citation Index
in Web of Science™ Core Collection (BKCI)

Interested in publishing with us?
Contact book.department@intechopen.com

Numbers displayed above are based on latest data collected.
For more information visit www.intechopen.com



Gamma Rays: Applications in Environmental Gamma Dosimetry and Determination Samples Gamma-Activities Induced by Neutrons

Hassane Erramli and Jaouad El Asri

Abstract

Gamma rays are high frequency electromagnetic radiation and therefore carry a lot of energy. They pass through most types of materials. Only an absorber such as a lead block or a thick concrete block can stop their transmission. In many alpha and beta transitions, the residual nucleus is formed in an excited state. The nucleus can lose its excitation energy and move to a “fundamental level” in several ways. (a) The most common transition is the emission of electromagnetic radiation, called gamma radiation. Very often the de-excitation occurs not directly between the highest level of the nucleus and its basic level, but by “cascades” corresponding to intermediate energies. (b) The gamma emission can be accompanied or replaced by the electron emission so-called “internal conversion”, where the energy excess is transmitted to an electron in the K, L or M shell. (c) Finally, if the available energy is greater than $2m_e c^2 = 1022 \text{ keV}$, the excited nucleus can create a pair (e^+ , e^-). The excess energy appears as a kinetic form. This internal materialization process is very rare. In this chapter we are presenting two applications of gamma rays: On the one hand, TL dosimeters and field gamma dosimetry are studied, a careful study of the correcting factors linked to the environmental and experimental conditions is performed. On the other hand, we are presenting a calculation method for controlling neutron activation analysis (NAA) experiments. This method consists of simulating the process of interaction of gamma rays induced by irradiation of various samples.

Keywords: gamma-ray, gamma attenuation, gamma spectroscopy, Monte Carlo simulation, medicine, industry, TL dosimetry

1. Introduction

The gamma rays are emitted from a nucleus or from the annihilation of positron with electrons. The most intense sources of gamma rays are radioactive sources. The photons resulting from de-excitation of nuclei have energies ranging from less than 1 to about 20 MeV.

The photons resulting from annihilations event can have much larger energy: the neutral pion (π^0), for example, produce two photons of about 70 MeV.

Gamma rays are ionizing electromagnetic radiation, obtained by the decay of an atomic nucleus. Gamma rays are more penetrating, in matter, and can damage living cells to a great extent. Gamma rays are used in medicine (radiotherapy), industry (sterilization and disinfection) and the nuclear industry. Shielding against gamma rays is essential because they can cause diseases to skin or blood, eye disorders and cancers.

The interaction of gamma rays with matter may be divided into three main categories depending on the energy of the photon. These three mechanisms are the photoelectric effect, Compton scattering and pair production. All results in the energy of the photon being transferred to electrons which subsequently lose energy by further interactions.

2. Origin of the gamma rays

The gamma radiations are constituted by photons, characterized by their energy, inversely proportional to their wavelength. The gamma rays come from the nuclei during the nuclear reactions, it is monoenergetics for a given characteristic reaction. So, the β -decay of the ^{137}Cs to ^{137}Ba produces a gamma radiation of 660 keV. The β -decay of the ^{60}Co to ^{60}Ni produces a double radiation emission of 1.17 and 1.33 MeV.

Natural gamma radiation sources can be easily divided into three groups according to their origin. The first group includes potassium (^{40}K) with a half-life of 1.3×10^9 years, uranium-238 (^{238}U) with a half-life of 4.4×10^9 years, uranium-235 (^{235}U) with a half-life of 7.1×10^8 years and thorium (^{232}Th) with a half-life of 1.4×10^{10} years.

The second group includes radioactive isotopes from the first group. Those have half-lives ranging from small fractions of a second to 10^4 to 10^5 years. The third group will include it isotopes created by external causes, such as the interaction of cosmic rays with the earth and its atmosphere.

2.1 Gamma radiation production mechanism

The Gamma rays are produced in number of ways:

- **Thermal radiation:** Only an extremely hot medium ($T = 10^8$ K) is likely to produce gamma radiation. Such media are extremely rare, and this process is not fundamental to the production of this radiation.
- **Inverse Compton effect:** During a collision with low energy photon, a relativistic electron can transfer to it a significant part of its energy, the photon can then have an energy of 100 MeV.
- **The Synchrotron radiation:** A relativistic electron spiraling through the force lines of a magnetic field radiates electromagnetic energy. Thus, energy electrons 3×10^8 MeV in a magnetic field of 3×10^{-6} Gauss will create a gamma radiation. But, by radiating the electrons lose energy: their lives are therefore limited.
- **Bremsstrahlung or braking radiation:** An electron passing near a nucleus is influenced by its Coulombian field. The deceleration of the electron is accompanied by a loss of energy in the form of gamma radiation when the electron has a relativistic speed.

- **Production of meson π^0 :** A meson can be produced during reactions of several types:
 - Collision between two protons or a proton and alpha (helium nucleus).
 - Collision between a proton and an antiproton; if the antimatter exists in the Universe, the observation of the gamma radiation produced is a method for detecting it. The meson (π^0) then disintegrates into two photons.
- **Nucleus de-excitation:** Just like an atom or a molecule, a nucleus has energy levels whose transitions between the least excited levels give rise to gamma radiation. Such nucleus de-excitation may occur either during the interaction of a nucleus with neutrinos or during certain thermonuclear reactions.

3. Gamma attenuation

Unlike charged particles that gradually loses up their energy to matter, when gamma rays traverse matter, some are absorbed, some pass through without interaction, and some are scattered as lower energy photons. Electromagnetic radiation vanishes brutally as a result of interaction. We can no longer talk about a slowdown. We have to introduce the attenuation notion.

Although a large number of possible interaction mechanisms are known, when monoenergetic gamma rays are attenuated in the matter, only four major effects are important: photoelectric effect, Compton effect, elastic or Rayleigh scattering and pair production (with a threshold energy of 1022 keV).

The probability which has a photon of energy given to undergo an interaction during the penetrating in a given material is represented by the attenuation coefficient for this material absorber. The more range of gamma rays in the absorber is long, the more the interaction probability increases. The attenuation coefficient is the sum of coefficients of the various interaction modes (Compton, photoelectric, pair production), the proportion of each of these effects varying with the radiation energy and nature of the absorber.

3.1 Attenuation law

When a narrow beam of N_0 (number of photons/unit area) monoenergetic photons with energy E_0 passes through an homogeneous absorber of thickness x , the number of photons that reach a depth (in cm) without having an interaction is given by:

$$N = N_0 e^{-\mu(\rho, Z, E)x} \quad (1)$$

where μ (in cm) is the linear attenuation coefficient for material of physical density (in g/cm³) and atomic number Z .

The total linear attenuation coefficient can be decomposed into the contributions from each above described mode of photon interaction as:

$$\mu_{tot} = \mu_{ph} + \mu_C + \mu_{coh} + \mu_p \quad (2)$$

where μ_{ph} , μ_C , μ_{coh} and μ_p are the attenuation coefficient for photoelectric effect, Compton scattering, Rayleigh scattering and pair production respectively. Although linear attenuation coefficients are convenient for engineering applications and

shielding calculations, they are proportional to the density of the absorber, which depends on the physical state of the material.

The relationship (1) can be written as:

$$N = N_0 e^{-\left(\frac{\mu(Z, \rho)}{\rho}\right) \rho x} \quad (3)$$

where μ/ρ (in cm^2/g) is the mass attenuation coefficient.

If the absorber is a chemical compound or mixture, its mass attenuation coefficient μ/ρ can be approximately evaluated from the coefficients for the constituent elements according to the weights sum

$$\left(\frac{\mu}{\rho}\right)_{\text{compound}} = \sum_i \left(\frac{\mu}{\rho}\right)_i w_i \quad (4)$$

where w_i is the proportion by weight of the i th constituent the material.

The mass attenuation coefficient of a compound or a mixture can be, therefore, calculated from the mass attenuation coefficient of the components [1].

The total linear attenuation coefficient, $\mu_{\text{compound or mixture}}$ of the compound or mixture can then be simply found by multiplying the total mass attenuation coefficient, $(\mu/\rho)_{\text{compound}}$ with its density, ρ . Thus,

$$\mu_{\text{compound}} = \left(\frac{\mu}{\rho}\right)_{\text{compound}} \times \rho \quad (5)$$

Figure 1 shows the linear attenuation of solid sodium iodide, a common material used in gamma-ray detectors.

3.2 Attenuation coefficients versus atomic number and physical density

The total mass attenuation coefficient μ/ρ is also proportional to the total cross section per atom σ_{tot}^2 . His relation is:

$$\frac{\mu}{\rho} = \sigma_{\text{tot}}^2 \left(\frac{\text{cm}^2}{\text{atom}}\right) \cdot \left(\frac{N_A}{A}\right) \left(\frac{\text{atoms}}{\text{g}}\right) \quad (6)$$

where $N_A = 6.03 \times 10^{23}$ is Avogadro's number and A is the atomic mass of the absorber (in g).

Since there are Z electrons per atom:

$$\frac{\mu}{\rho} = \sigma_{\text{tot}}^2 \cdot \left(\frac{ZN_A}{A}\right) = \sigma_{\text{tot}}^2 \cdot \delta_e$$

where σ_{tot}^2 ($\text{cm}^2/\text{electron}$) is the total cross section per electron and the term $\left(\frac{ZN_A}{A}\right)$ represents the electron density (number of electrons per g).

For all elements except hydrogen, δ_e approximately equals $N_A/2 = 3 \times 10^{23}$, because $Z/A = 1/2$. For hydrogen, δ_e is equal to N_A , and is therefore twice the « normal » value.

This indicates that atomic composition dependence of $\frac{\mu}{\rho}$ is uncorrelated to the term δ_e , and is related to the term σ_{tot}^2 . The linear attenuation coefficient μ is, therefore, approximately depending on Z in the physical density term ρ and expressly depending on Z in term σ_{tot}^2 .

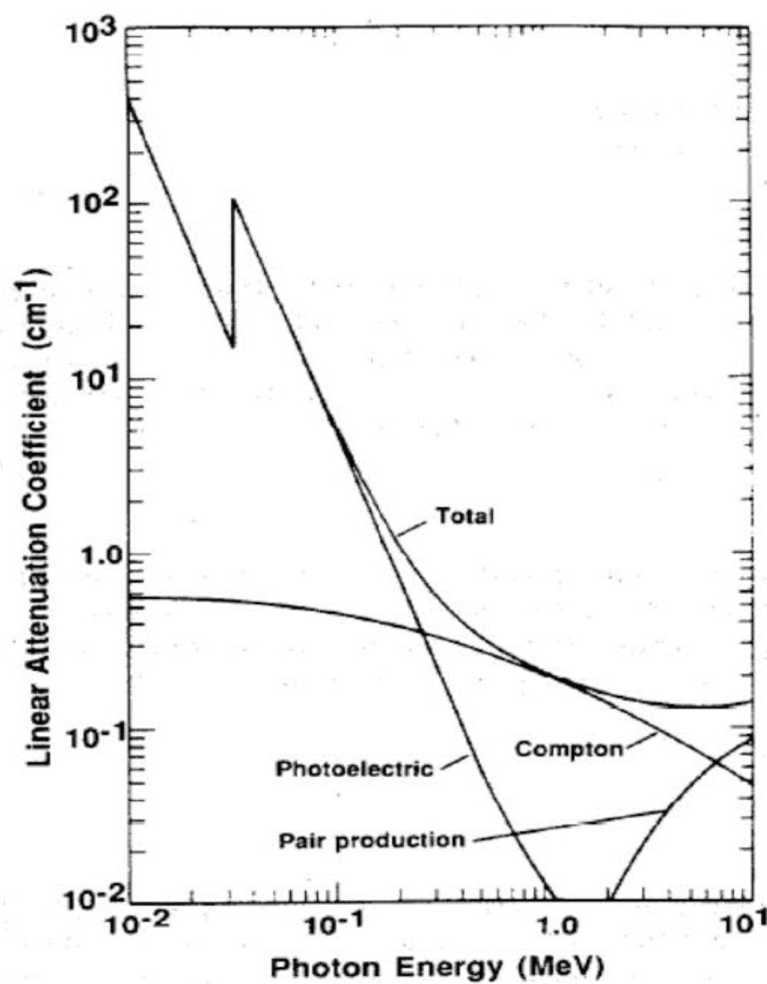


Figure 1.
 Linear attenuation coefficient of NaI showing contributions from photoelectric absorption, Compton scattering, and pair production [2].

3.3 Calculation of HVL, TVL and relaxation length (λ)

The linear attenuation coefficient is inversely proportional to a quantity called a half-value layer (HVL), which is the material thickness needed to attenuate the intensity of the incident photon beam to half of its original value. This means that when $x = \text{HVL}$, $\frac{N_0}{N} = \frac{1}{2}$.

From Eq. (3) it can be shown that:

$$\begin{aligned} \frac{N_0}{2} &= N_0 e^{-\mu \text{HVL}} \\ \text{HVL} &= \frac{\ln 2}{\mu} = \frac{0.693}{\mu} \end{aligned} \tag{7}$$

The HVL of a given material thus characterizes the quality (penetrance or hardness) of a gamma beam.

Figure 2 shows the relationship between the linear attenuation coefficient and the HVL for a soft tissue [3].

3.4 Calculation of relaxation length (λ)

The average distance between two successive interactions is called the relaxation length (λ) or the photon mean free path which is determined by the equation:

$$\lambda = \frac{\int_0^\infty x e^{-\mu x} dx}{\int_0^\infty e^{-\mu x} dx} = \frac{1}{\mu} \tag{8}$$

where μ is the linear attenuation coefficient and x is the absorber thickness.

N.B: The relaxation length is the thickness of a shield for which the photon intensity in a narrow beam is reduced to $1/e$ (or 0.37) of its original value.

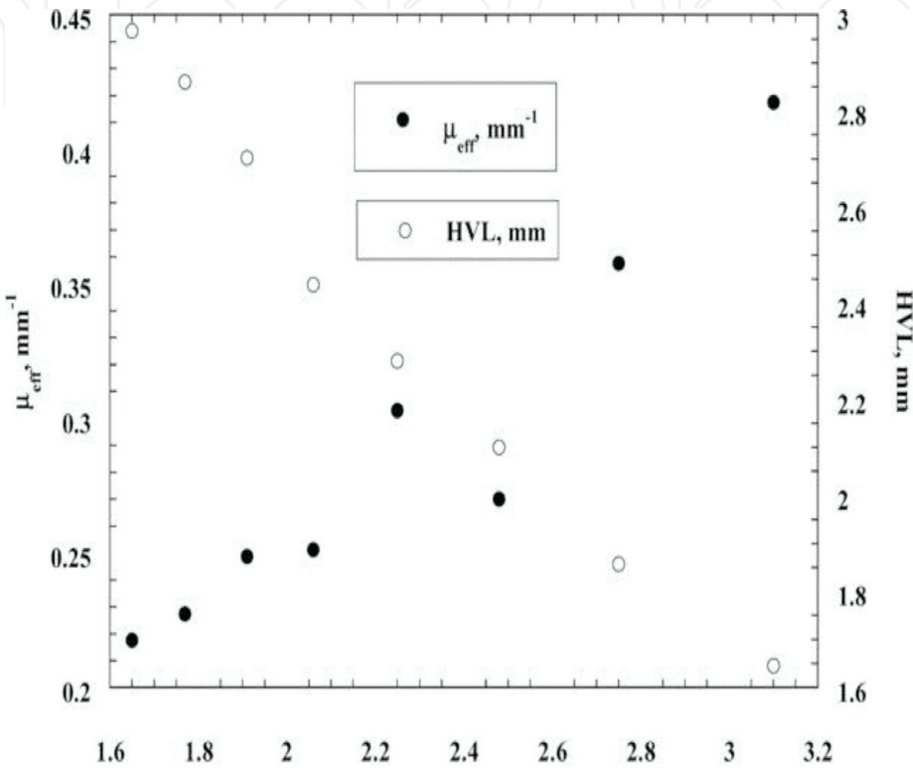


Figure 2.
Relationship between the linear attenuation coefficient and the HVL for a soft tissue.

4. Application field

Apart from the use of nuclear energy for the supply of electricity, the applications of radioactivity are numerous in many areas: medical physics, earth sciences, industry and preservation of cultural heritage.

The properties used for these various applications are:

- Time decline of radioactivity
- Radiation emission
- Sensitivity of detection

4.1 Medical physics applications

The major application of radiation in medicine is radiotherapy and/or treatment by ionizing radiation. A few months after the discovery of X-rays, there is over a century, it has become clear that biological action radiation could be used in the

treatment of cancers. Cancers cells divided more quickly are more sensitive, than normal cells to ionizing radiation. By sending these cells a certain dose of radiation, it is possible to kill them and eliminate the tumor.

4.2 Sterilization of objects by gamma radiation

- **Irradiation of surgical and food material:** Irradiation is a privileged means to destroy micro-organisms (fungi, bacteria, virus...). As a result, many applications radiation exists for sterilization of objects. For example, most medical-surgical equipment (disposable syringes, etc.) is today radio-sterilized by specialized industrialists. Similarly, the treatment by irradiation of food ingredients allows improve food hygiene: sterilization spices, elimination of salmonella from shrimp and frog legs. This technics is also known as food ionization.
- **Irradiation of art objects:** Treatment with gamma rays helps to eliminate larvae, insects or bacteria lived inside objects, to protect them from degradation. This technics is used in the treatment of conservation and restoration of arts objects, ethnology and archaeology. It is applicable to different types of materials: wood, stone, leather, etc.

4.3 Industrial applications

- **Elaboration of materials:** Irradiation causes, under certain conditions, chemical reactions that allow the development of more resistant materials, more lightweight, capable of superior performance.

4.4 Gamma rays spectrometry

The development of γ -spectrometry began with the development of nuclear sciences and technology to meet the needs for the control, characterization and analysis of radioactive materials. This measurement technics exploits a fundamental property observed for unstable nuclei: the emission of radiation from the process of nuclear decay. It is thus known as non-destructive because it respects the integrity of the object to be analyzed [4].

The interest in γ spectrometry has continued to grow over the years, both from a point of view metrological and a point of view applications. This development was made possible by a better understanding of the process of photon interaction with matter, and especially by the appearance of semiconductor detectors in the 1960s. Spectrometry γ then became a powerful tool for studying decay patterns. It is now used in a wide variety of sectors (for example: dating, climatology, astrophysics, medicine) and in virtually all stages of the fuel cycle.

Photon spectrometry is a commonly used nuclear measurement technique to identify and quantify gamma emitting radionuclides in a sample. It is non-destructive and does not require specific sample preparation. Conventional spectrometers are designed around semiconductor detectors, usually with high purity germanium (hyper-pure germanium).

The radionuclides measured by this method emit gamma photons of specific energies and their interactions with the detector depend on several variables (geometry or conditioning: physical shape of the object, density, measured quantity, container type, emission energy, size, shape, nature of the detector, etc.).

5. Example of gamma rays applications

5.1 Environmental gamma dosimetry

The thermoluminescence dating method (TL) requires a very accurate knowledge of the annual radiation doses deposited, in the minerals that are used, by the alpha, beta, gamma and cosmic rays [5, 6].

In the annual radiation doses, we can distinguish two components:

- internal dose: deposited by the radiations with a short range (alpha and beta) coming out of the bulk of the sample.
- external dose: deposited by the long range radiations (gamma rays and cosmic) coming out of the surroundings of the sample.

Gamma-ray dose-rate may be measured by a TL dosimeter. But as this dose is not valid for the dosimeter itself, corrections must be made to know the one corresponding to the soil.

These corrections are related to the complexity of the energy spectrum gamma radiation incidents; their origins are:

- The difference in composition between TL dosimeter and the soil, resulting in absorption and therefore deposited different doses, especially for an energies less than 100 keV.
- The capsule enclosing the TL dosimeter induce absorptions of low energy gamma rays.

The correction factors had already been investigated theoretically [7] and experimentally [8, 9]. Below, we describe a theoretical evaluation method, for these factors, which does not require excessive computer time and so can be easily extended to a wide variety of site conditions.

5.1.1 Environmental conditions

The calculations presented here refer to CaSO_4 : Dy as dosimeter, and two encapsulating materials, polyethylene and copper, of various thicknesses (**Figure 3**). However, the resulting computer programs can be easily extended to other materials.

Several kinds of soils were considered. For this case, we retained two extreme cases of real soils:

- a siliceous soil of low $\langle Z \rangle$ ($\langle Z \rangle = 11.26$), hereafter referred to as ‘S soil’;
- a very calcareous soil of high $\langle Z \rangle$ ($\langle Z \rangle = 14.07$) referred to as ‘C soil’.

The relative energies and intensities of the lines taken into consideration are given in **Table 1** [10]. For the uranium series, the contribution of uranium-235 and its descendants were taken into account.

The bulk of the calculation therefore comes down to a few dozen successive numerical integrations, with about 220 steps each time. It is therefore a much

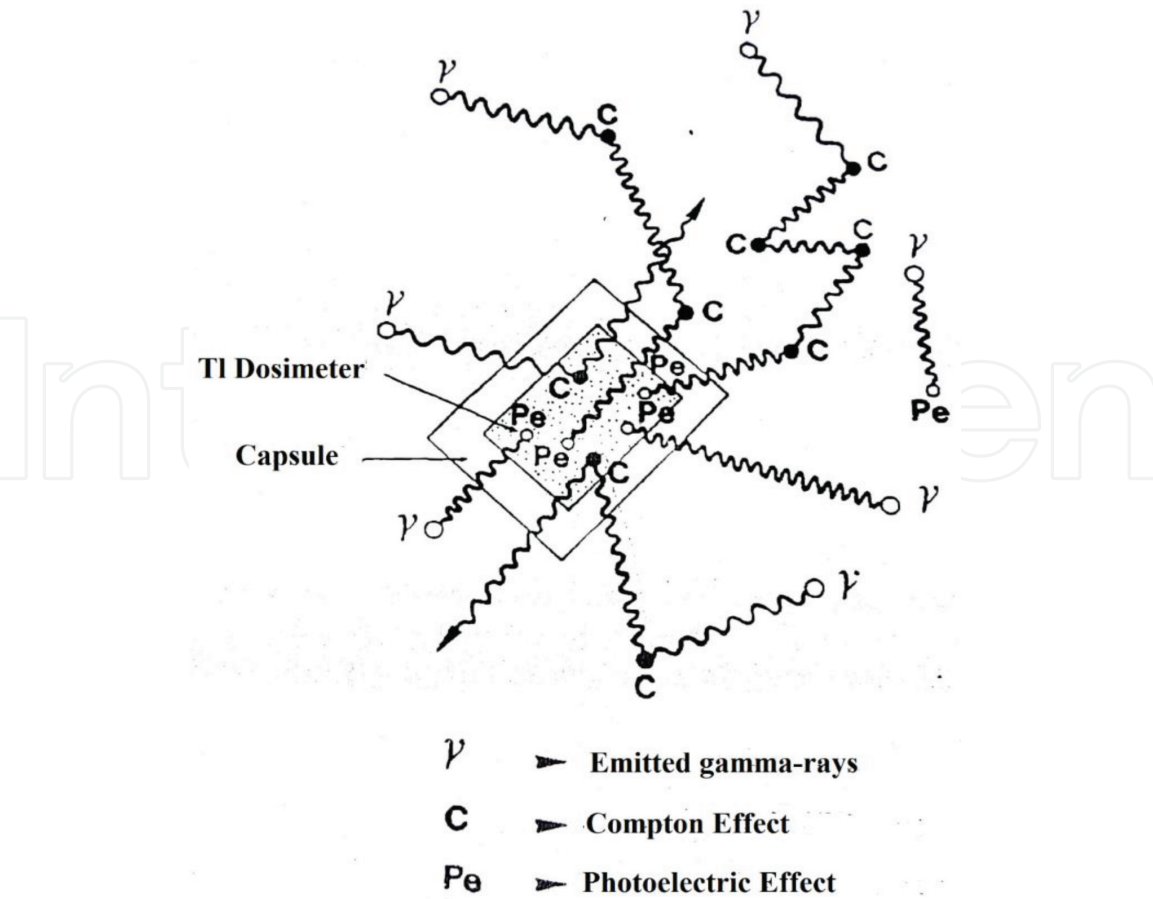


Figure 3.
TL dosimeter irradiated by an incident γ -ray flux.

lighter and less demanding procedure in computer time than the Monte-Carlo method for a similar definition.

5.1.2 Outline of the calculations of the dosimeter/soil dose ratio

The ratio ε of the dose deposited in an encapsulated dosimeter by an incident gamma flux to that deposited in soil by the same flux can be evaluated using the expression:

$$\varepsilon = \frac{\int \phi(E) E \mu_{a1} \cdot e^{-\mu_{a2} t} dE}{\int \phi(E) E \mu_{a3} dE} \tag{9}$$

where E is the photon energy: $\phi(E)$ is the incident γ -ray flux density (γ per unit area and unit time); μ_{a1} , μ_{a2} , μ_{a3} are the total mass absorption coefficients for γ -rays, respectively in dosimeter, capsule walls, and soil; t is the capsule thickness.

In fact, formula Eq. (9) is only approximate and a more exact formulation is:

$$\varepsilon = \frac{\int E \mu_{a3} \{ (1 - e^{-\mu_{02} t}) \phi(E) + \int e^{-\mu_{02} t} \cdot \left(\frac{\sigma_{02}}{\mu_{02}} \right) F(E, E') \phi(E') dE' \} dE}{\int \phi(E) E \mu_{a3} dE} \tag{10}$$

where μ_{02} and σ_{02} are, respectively the total and Compton mass attenuation coefficients for the encapsulating material; $F(E, E')$ is the energy distribution of secondary γ -rays (energy E') from a Compton interaction induced by a photon of

Energy (keV)	Intensity	Energy (keV)	Intensity
²³⁸ U + ²³⁵ U			
13	90	768	9
49	30	934	5
75	22	1120	17.5
92	14	1238	8
186	7	1377	8.6
242	10	1509	4.4
295	21	1764	23.3
352	40	2204	8.2
609	49		
²³² Th			
12	79	511	8.6
77	30	583	32.6
87	16	727	7.2
129	7	795	8.5
209	6	911	30
239	48	969	25.4
277	10	1588	11.6
338	16.4	2615	35.8
463	7		

Table 1.
U and Th series γ spectra.

energy E . $F(E, E')$ can be obtained from the well-established Klein and Nishina cross-section for Compton effect [11].

For the use of these formulas, it is assumed that there is an electronic equilibrium, that is, the dimensions of the dosimeter are equal to or greater than the secondary electron range (of the order of a few mm). Murray [9] showed that this is verified if the dosimeter mass is greater than 100 mg.

In applying formula Eq. (9), the main difficulty lies in the calculation of the incident photon flux density $\phi(E)$. $\phi(E)$ includes not only the discrete primary emission spectrum of the considered γ source, but also the continuum spectrum of γ rays from successive Compton interactions.

5.1.3 Infinite medium γ -ray spectrum

Here one assumes an infinite environment and homogeneous, in which the radio-elements are evenly distributed. The interactions of gamma rays with the material taken into consideration are the photoelectric effect and the Compton effect; the pair production is considered negligible to the considered energies (<2.6 MeV).

Let $N_0(E)$ be the primary spectrum (number of photons per unit time and unit mass of soil). After one interaction, the energy spectrum of secondary γ -rays will be:

$$N_1(E') = \int N_0(E) \frac{\sigma_{01}(E)}{\mu_{01}(E)} F(E, E') dE \tag{11}$$

And the ratio of secondary to primary γ -rays is:

$$Q_1 = \frac{\int N_0(E) \cdot \left(\frac{\sigma_{01}}{\mu_{01}}\right) \cdot dE}{\int N_0(E) \cdot dE} \tag{12}$$

In the same way, the spectrum of third generation γ -rays can be deduced from $N_2(E)$, and in a more general manner the following recurrence relations hold:

$$N_i(E') = \int N_{i-1}(E) \cdot \frac{\sigma_{01}(E)}{\mu_{01}(E)} F(E, E') dE \tag{13}$$

And the total spectrum will be:

$$N(E) = \sum_{i=1}^{\infty} N_i(E) \tag{14}$$

Of course, there is a rapid decrease with i of the mean γ energy and of the total energy carried.

Figure 4 an example of various order spectra for ^{40}K .

Practically, the calculation will be stopped at a generation order i such that $Q_i \ll 1$. The condition $Q_i < 10^{-3}$ was imposed, corresponding to $i = 15\text{--}32$ according to the medium involved.

$N(E)$ is the photon spectrum corresponding to the number of photons created per unit mass; to get $\phi(E)$, which is the number of incident photons per unit area, the mean relaxation length $\lambda(E)$ of photons must be taken into account:

$$\phi(E) = \lambda(E) \cdot N(E) = \sum \frac{N_i(E)}{\mu_{01}} \tag{15}$$

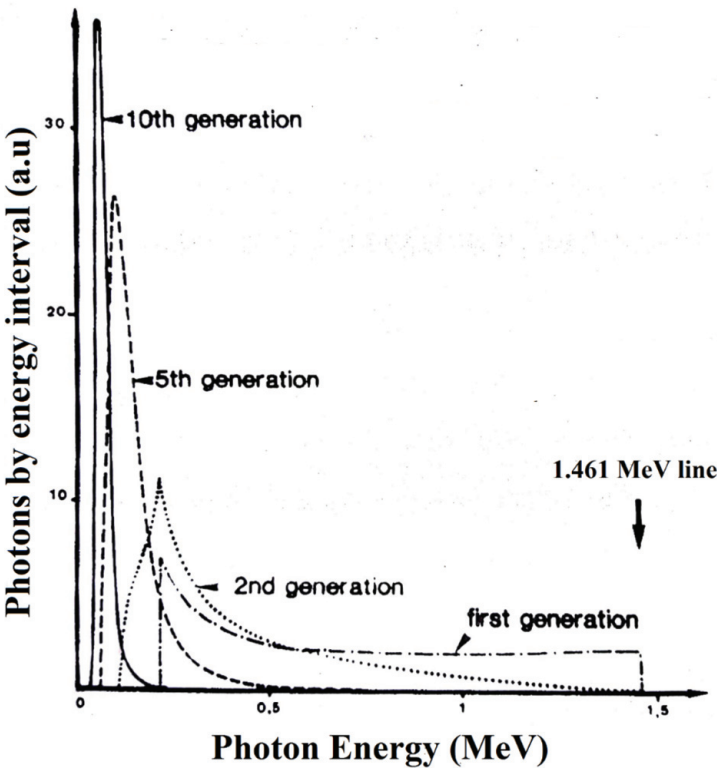


Figure 4.
Computed spectra of secondary γ -rays from ^{40}K after 1, 2, 5, 10 Compton interactions [5].

$$(\text{With}) : \lambda(E) = \frac{1}{\mu_{01}}$$

The value of absorption or attenuation coefficients was obtained for the Compton effect from the Klein-Nishina formula.

For the photoelectric effect, they were deduced from the data of Hubbell [12].

Some typical spectra are shown in **Figure 5** for ^{40}K . The low energy cut-off is determined by photoelectric effect and occurs at higher energy for high-Z media. And for ^{232}Th in pure water (**Figure 6**).

In the case of water, a “light” medium and a strong low energy ray contribution (below 100 keV) can be noticed. Similar features are also noticed for the more complex case of U and Th series.

These spectra show the overlapping of the primary ray spectrum and the degraded continuous spectrum, which carry most of the energy (60%).

There is a similarity in the degraded spectrum, even for two very different gamma sources (for example, thorium and potassium-40). On the other hand, the degraded spectrum is higher in energy as the $\langle Z \rangle$ of the medium is high: this is due to the increasing influence of the photoelectric effect which “cuts” the low gamma ray energy.

Our results are in good agreement with those obtained by G. Valladas [7] by the Monte-Carlo method for potassium-40 in siliceous medium.

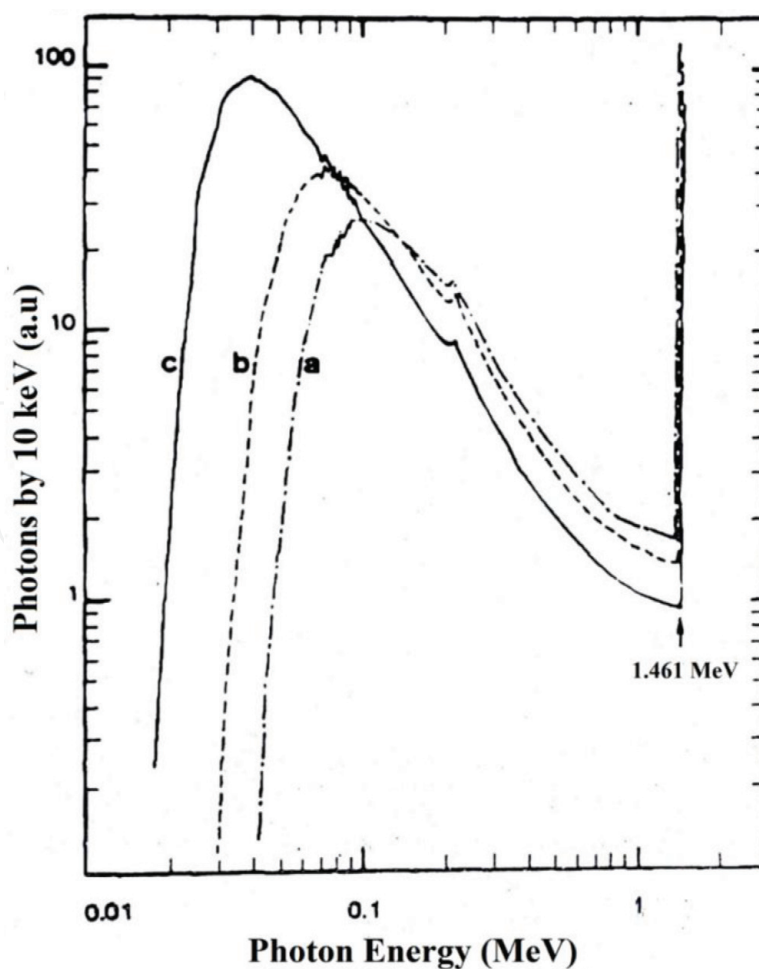


Figure 5.
Computed energy spectra for ^{40}K in (a) dry C soil, (b) wet S soil, and (c) pure water [5].

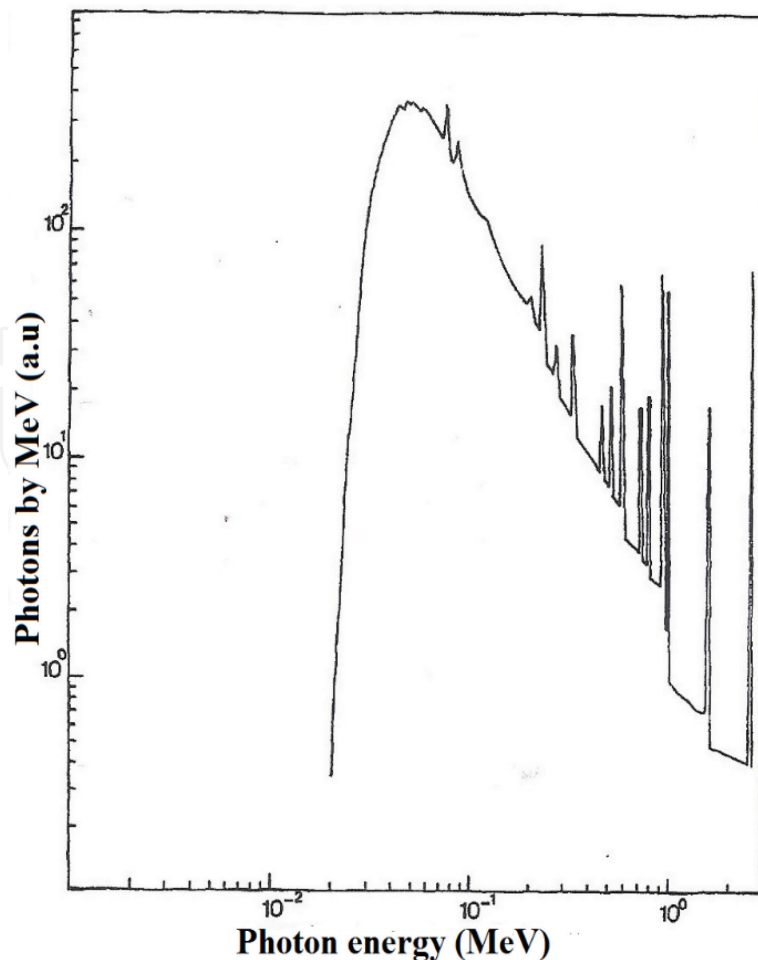


Figure 6.
Computed energy spectra for ^{232}Th in pure water [5].

5.1.4 Dosimeter to soil dose ratio for infinite homogeneous soils

The calculation of ϵ was done for the list of floors already cited (from the gamma ray energy spectra already calculated), for the three radiation sources and for two types of 1 g/cm^2 thick absorbers, sufficient to stop beta radiation.

- Copper, $\langle Z \rangle$ medium, frequently used
- Polyethylene, $\langle Z \rangle$ low

The results are given in **Table 2**. Calculations are performed here with, as a TL dosimeter, $\text{CaSO}_4:\text{Dy}$, but are readily feasible for any combination of known dosimeters and compositions.

It can be found that ϵ it may be less than or greater than 1; two antagonistic effects act: on the one hand, the absorption by the walls, which tends to decrease ϵ on the other hand, the difference in nature between soil and TL dosimeter which has the opposite effect, the coefficient of absorption of the dosimeter being the highest.

The dispersal of the value of ϵ is smaller between the different soil for a copper capsule than for a polyethylene capsule. This can be explained by the fact that copper absorbs the lower part of the spectrum of energy for which the difference dose between the dosimeter and the soil is significant.

Surrounding media	⁴⁰ K		Uranium		Thorium	
	Encapsulating		Encapsulating		Encapsulating	
	Polyethylene	Copper	Polyethylene	Copper	Polyethylene	Copper
C soil	0.96	0.95	0.94	0.89	0.95	0.91
C soil + 15% water	0.97	0.95	0.96	0.90	0.96	0.91
S soil	1.03	0.97	1.10	0.95	1.08	0.96
S soil + 15% water	1.05	0.98	1.13	0.96	1.11	0.97
S soil + 30% water	1.06	0.98	1.16	0.97	1.14	0.98
S soil + 50% water	1.07	0.96	1.20	0.95	1.17	0.96
Pure water	1.35	1.01	1.82	1.03	1.70	1.03

Table 2.
Values of ϵ for infinite uniform medium with 1 g m^{-2} capsule wall thickness [5].

For a copper capsule, the difference of ϵ between dry a soil and moderately wet (e.g., less than 15% water) is negligible (less than 1%); therefore, it is not necessary in this case to know exactly the soil humidity to perform the correction, which is an advantage.

In practice, the limestone soil and the siliceous soil are two extreme cases, which make only a difference of 5% for copper on the value of ϵ , so only a coarse knowledge of the casing medium is necessary for the calculation of ϵ with an high accuracy.

The variations of ϵ for ⁴⁰K with the absorber or medium are less important than for uranium or thorium. This is due to a smaller contribution of low energies to the ⁴⁰K spectrum (no low energy lines).

An important consequence of the foregoing is that, for the experimenter, copper (or a close material) is well used when the composition (especially moisture) of the soil is not well known. The error made a priori on the value of ϵ will thus be reduced.

On the other hand, in most cases, the dispersion on ϵ related to the relative intensity of the three gamma radiation sources is insignificant. Indeed, the potassium-40, uranium and thorium series generally intervene for approximately 1/3 each, and significant deviations from this proportion are rare.

In general, it is difficult to determine the respective contribution of the potassium-40, uranium and thorium series to the total dose rate. However, in most cases, the contribution of these three radioelements does not exceed 60% and approximate values on the whole with acceptable dispersion may be proposed.

For example,

- $\epsilon = 0.97 \pm 0.01$ for S soil + 15% water
- $\epsilon = 0.92 \pm 0.01$ for dry C soil.

The results obtained with our program under the same conditions regarding the dosimeter, the surrounding environment, the capsules and the sources of the gamma rays are slightly superior to the theoretical results of G. Valladas [7]. This small difference (in the order of 3%) can be explained by the fact that the nominal values for capsule thickness have been used instead of the mean values which take into account geometry, also to a lesser extent by the fact that self-absorption has not been taken into account in our calculation. The effect of this last correction was estimated to be less than 1%.

5.2 Calculation method adapted to the experimental conditions for determining samples γ -activities induced by 14 MeV neutrons

5.2.1 Introduction

The gamma radiation self-absorption coefficient is of great interest in activation analysis. Since it is difficult to measure this coefficient, various calculation methods have been developed.

Measuring the self-absorption coefficient is not a simple thing. The physicists who have faced this problem, for a long time, have always used methods of statistical or non-statistical computation: Parallel beam methods, Monte-Carlo method and many other methods. For our part, we have developed an original technique calculating the self-absorption coefficient of multienergetic γ -radiations [13].

In this chapter, we are presenting a method that we have developed, this which allows us control and calibrate the activation analysis experiments [13]. This method consists of simulating the interaction processes of gamma rays induced by neutron activation of various samples by using the Monte Carlo method adapted to experimental conditions.

5.2.2 Samples and standards induced gamma-activities

Different disk shaped red beet samples and standards were irradiated with 14 MeV neutrons. Standards were prepared by mixing pure graphite and high purity chemical compounds powders (NaCl, Na₂HPO₄ and K₂CO₃) [14]. The induced gamma activities on the sodium, potassium, chlorine and phosphorus elements have been experimentally measured by means of hyper-pure germanium spectrometer.

The analyzed beet samples and standards have a 23 mm diameter and a 6 mm thickness.

The different parameters of the nuclear reactions used (cross section, isotopic abundance, etc.) are summarized in **Table 3**.

After the irradiation (irradiation time = t_{irr}) and cooling times (t_d), the number of produced radionuclides is given by:

$$N(t_{irr} + t_d) = \frac{TN_0\sigma\phi}{\ln 2} \theta I_\gamma \left(1 - e^{-\left(\frac{\ln 2}{T}\right)t_{irr}}\right) \cdot e^{-\left(\frac{\ln 2}{T}\right)t_d} \tag{16}$$

where σ is the nuclear reaction cross section, N_0 is the number of target nuclei, T is the half-life of the produced radionuclide, θ is the isotopic abundance of the studied element, I_γ is the emitted gamma rays intensity and ϕ the neutron flux. To take into account the activity measuring time, relation Eq. (16) should be multiplied by the term $\left(1 - e^{-\left(\frac{\ln 2}{T}\right)t_m}\right)$.

Element	θ (%)	Nuclear reaction	σ (mb)	T	E_γ (keV) (I_γ %)	t_{irr} (s)	t_d (s)	t_m (s)
Na	100	$^{23}\text{Na}(n, p)^{23}\text{Ne}$	43 ± 5	38.0 s	440 (33%)	200	30	200
Cl	75.5	$^{35}\text{Cl}(n, 2n)^{34m}\text{Cl}$	43 ± 5	32.4 min	146.5 (45%)	600	30	600
P	92.2	$^{31}\text{P}(p, \alpha)^{28}\text{Al}$	43 ± 5	2.30 min	1779 (100%)	600	30	600
K	93.1	$^{39}\text{K}(n, 2n)^{38g}\text{K}$	43 ± 5	7.70 min	2167 (100%)	600	30	600

Table 3.
The produced nuclear reactions by irradiating the samples (standards) with 14 MeV neutrons.

5.2.3 Calculation method

The transmission probability of a gamma photon generated from point P_1 (**Figure 7**) after crossing a path length $l_1 = P_1S_1$ in a homogeneous disk shaped sample (standard) of radius R_1 in cm, depth D in cm, and density ρ_1 in g.cm^{-3} is given by:

$$P(l_1) = e^{-\mu_1 l_1}$$

where μ_1 is the total attenuation coefficient of the gamma rays in the irradiated sample.

The interaction probability of a gamma photon after crossing a path $l_2 = Q_2S_2$ (**Figure 7**) in a disk shaped detector of radius R_2 in cm, depth e in cm and density ρ_2 in g.cm^{-3} is given by:

$$P(I_2) = (1 - e^{-\mu_2 l_2}) \quad (17)$$

where μ_2 is the total attenuation coefficient of the gamma photon in the detector. The absorption probability of a gamma photon in the detector is given by:

$$P = e^{-\mu_1 l_1} (1 - e^{-\mu_2 l_2}) \quad (18)$$

Consequently the detection rate for N photons is:

$$\bar{\omega} = \frac{1}{N} \sum_{i=1}^N e^{-\mu_1 l_{1i}} (1 - e^{-\mu_2 l_{2i}}) \quad (19)$$

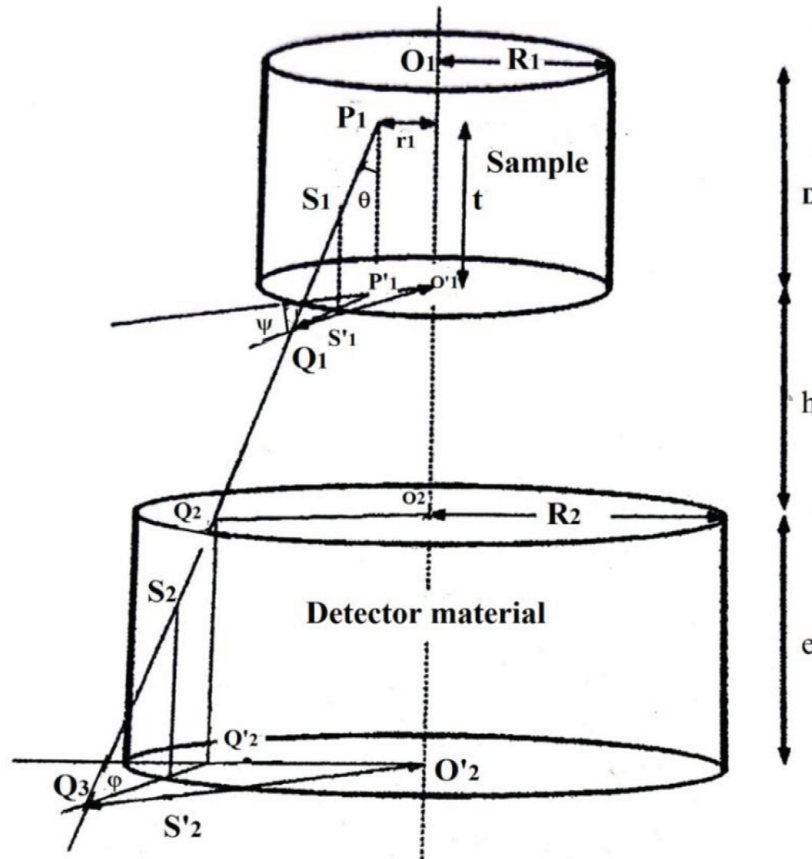


Figure 7.
The irradiated sample (standard) to γ -detector arrangement used in the activities calculation.

By combining relations Eq. (16) and Eq. (19) we get the number of the detected gamma rays.

$$N_c = \frac{TN_0\sigma\phi}{\ln 2} \theta I_{\gamma} \overline{\omega} \left(1 - e^{-\left(\frac{\ln 2}{T}\right)t_{irr}}\right) \cdot e^{-\left(\frac{\ln 2}{T}\right)t_d} \cdot \left(1 - e^{-\left(\frac{\ln 2}{T}\right)t_m}\right) \quad (20)$$

The total attenuation coefficients are calculated by using respectively the Klein-Nishina theory formula [12], Allen Brodsky's approximation [15], and Max Born's approximation [16], for the Compton, photoelectric and pair production effects.

The calculation of the paths lengths l_1 and l_2 consists firstly on generating random numbers by using a programme based on a congruentia 1 method.

The path length l_1 is given by [17]:

$$l_1 = \begin{cases} \frac{t}{\cos\theta} & \text{if } R_1 \geq \overline{O'_1O_1} \\ l(r, \theta, \psi) & \text{if } R_1 < \overline{O'_1O_1} \end{cases}$$

where:

$$\overline{O'_1O_1}^2 = r_1^2 + t^2 \cdot \tan^2(\theta) + 2r_1 \cdot t \cdot \tan(\theta) \cdot \cos(\psi)$$

$$\text{And : } l(r, \theta, \psi) = \frac{\sqrt{R_1^2 - r_1^2 \sin^2(\psi)} - r_1 \cos(\psi)}{\sin(\theta)}$$

The uniform random sampling of the emission point P_1 and emission direction is achieved by computing the distance from the center r_1 , the depth t , $\cos(\theta)$ and ψ , with four uniform random numbers [17]:

$$r_1 = R_1 \sqrt{\xi_1}$$

$$t = D\xi_2$$

$$\cos(\theta) = \xi_3$$

$$\psi = 2\pi\xi_4$$

$$(\text{With}) 0 \leq \xi_i \leq 1$$

We have developed the following theory to calculate the path length l_2 which is given by:

$$\begin{cases} 0 & \text{if } R_2 \leq \overline{O_2Q_2} \\ \frac{e}{\cos\theta} & \text{if } R_2 > \overline{O_2Q_2} \text{ and } R_2 \geq \overline{O'_2Q_3} \\ X_2 & \text{if } \overline{O_2Q_2} < R_2 < \overline{O'_2Q_3} \end{cases}$$

where

$$\overline{O_2Q_2}^2 = r_1^2 + (t+h)^2 \cdot \tan^2(\theta) + 2r_1 \cdot (t+h) \cdot \tan(\theta) \cdot \cos(\psi)$$

$$\overline{O'_2Q_3}^2 = r_2^2 + e^2 \cdot \tan^2(\theta) + 2r_2 \cdot e \cdot \tan(\theta) \cdot \cos(\psi)$$

h is the distance between the sample and the detector (**Figure 7**). r_2 is the distance from the axis of the detector and:

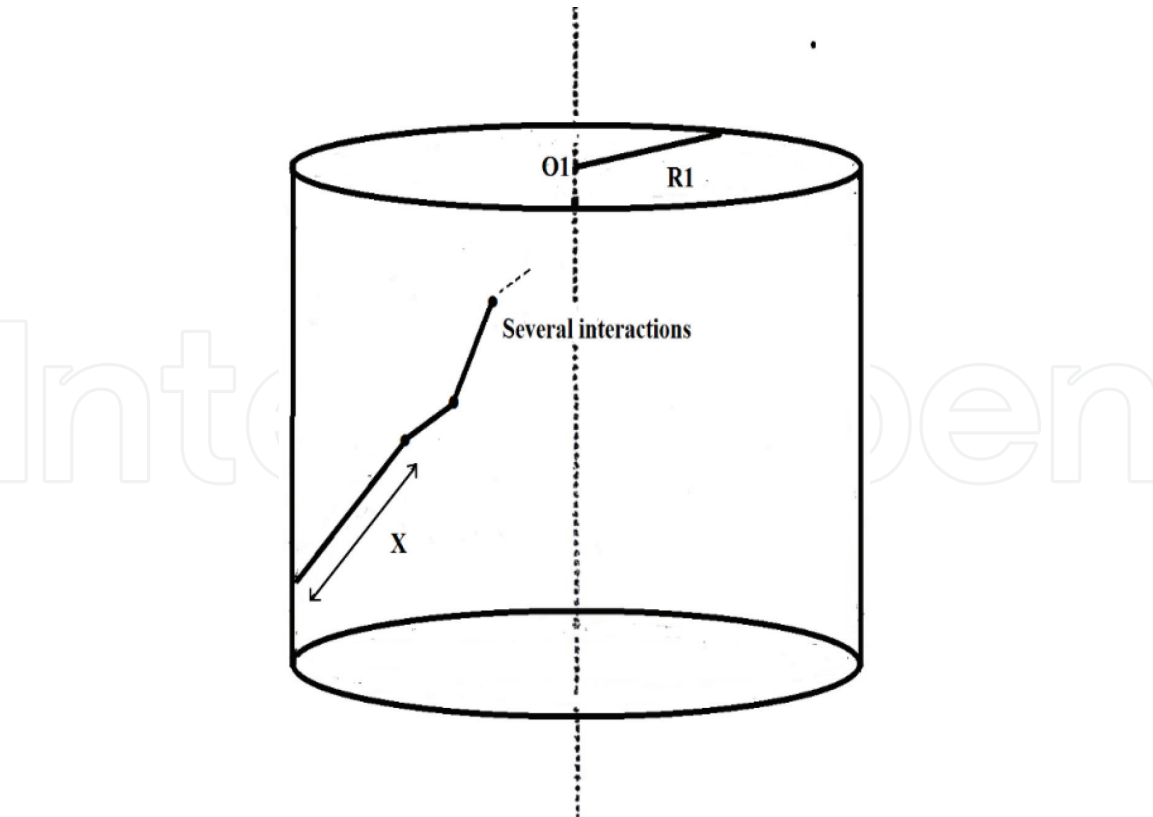


Figure 8.
Scheme shows changes in gamma-ray direction in the case of multiple interactions.

$$X_2 = \begin{cases} 0 & \text{if } \tan \theta \geq \tan \theta_{\max} \\ \frac{\sqrt{R_2^2 - r_2^2 \sin^2 \varphi} - r_2 \cos \varphi}{\sin \theta} & \text{if } \tan \theta < \tan \theta_{\max} \end{cases}$$

(With) $\tan \theta_{\max} = \frac{R_2 - R_1}{t + h}$

To complete this study, we have developed another program based on the EGC method [18]. This program results in determining the energy loss predominant phenomenon that occurs when gamma rays interact with the absorber.

For this, we compare the range x to the relaxation length (λ) of the γ -rays in the material (**Figure 8**).

5.3 Results and discussions

The measured N_m and calculated N_c activities of some different irradiated standards containing Na, K, Cl, and P are shown in **Table 4**.

Element	Element mass (mg)	ϕ	N_m	N_c	$R = \frac{N_c}{N_m}$
Na	0.51	1.0×10^7	50 ± 7	58.0 ± 0.2	1.16
K	2.32	2.3×10^8	17 ± 4	14 ± 0.1	1
Cl	0.92	5.0×10^8	447 ± 21	432 ± 1	0.96
P	1.61	2.0×10^9	2533 ± 50	2700 ± 5	1.06

Table 4.
Data obtained for different irradiated standards with a 14 MeV neutron flux by experimental N_m and calculation N_c methods.

We notice that the results obtained by the two methods (experimental and calculation) are in good agreement with each other. The calculation method has the advantage of being accurate (error is smaller than 3%) and rapid (the calculation time is of about 2 min).

6. Conclusion

In the first part of the chapter, a careful study of the correcting factors linked to the environmental and experimental conditions is performed.

In the second part, the calculation method was developed. It is very accurate, rapid, adapted to the experimental conditions, it does not necessitate the use of a very expensive detection chain, and can be used to determine the trace element concentrations in materials. This technique is a good test for neutron activation analysis experiments. It allows these experiments to be calibrated in cases where it is difficult to achieve standards.

Author details


Hassane Erramli^{1*} and Jaouad El Asri²

¹ Faculty of Sciences Semlalia, University Cadi Ayyad, Marrakech, Morocco

² Nuclear Reactor and Nuclear Security, Faculty of Sciences, University Mohammed V, Rabat, Morocco

*Address all correspondence to: hassane@uca.ac.ma

IntechOpen

© 2019 The Author(s). Licensee IntechOpen. This chapter is distributed under the terms of the Creative Commons Attribution License (<http://creativecommons.org/licenses/by/3.0>), which permits unrestricted use, distribution, and reproduction in any medium, provided the original work is properly cited. 

References

- [1] McCullough EC. Photon attenuation in computed tomography, Medical Physics. 1975;6:307
- [2] Hubbell JH. Photon cross sections, attenuation coefficients, and energy absorption coefficients from 10 keV to 100 GeV. National Bureau of Standards report NSRDS-NSB 29; August 1969
- [3] AL-Akhras M-A, Aljarrah K, Omari AH, Khateeb HM, Albiss BA, Azez K, et al. Influence of extremely low energy radiation on artificial tissue: Effects on image quality and superficial dose. Spectroscopy. 2008;22(5):419-428
- [4] Lyoussi A. Mesure nucléaire non destructive dans le cycle du combustible. Techniques de l'Ingénieur, Réf. BN3405; Janvier 2005
- [5] Erramli H. Développement de la dosimétrie appliquées à la datation par thermoluminescence [PhD thesis]. France: Université Blaise Pascal; 1986
- [6] Fain J, Erramli H, Miallier D, Montret M, Sanzelle S. Environmental gamma dosimetry using TL dosimeters: Efficiency and absorption calculations. Nuclear Tracks. 1985;10(4-6):639-646
- [7] Valladas G. Mesure de la dose γ annuelle de l'environnement d'un site archéologique par un dosimetre TL. Photodynamic Antimicrobial Chemotherapy. 1982;6:77-85
- [8] Mejdahl V. Measurement of environmental radiation at archaeological sites by means of TL dosimeters. Photodynamic Antimicrobial Chemotherapy. 1978;2:70
- [9] Murray AS. Environmental radiation studies relevant to thermoluminescence dating [PhD thesis]. Oxford; 1981
- [10] Ewbank WB. Status of transactinium nuclear structure data. In: The Evaluated Nuclear Structure Data File. IAEA-TECDOC-232. Vienna: International Atomic Energy Agency; 1980. pp. 109-141
- [11] Evans RD. Gamma rays. In: American Institute of Physics Handbook. New York: McGraw-Hill; 1972. pp. 8-190-8-218
- [12] Hubbell JH. Photon cross-sections attenuation coefficients and energy absorption coefficients for 10keV to 100GeV photons, NSRD-NBS-29. Washington; VS Government Printing Office; 1969
- [13] Rzama A, Erramli H, Misdaq MA. A new calculation method adapted to the experimental conditions for determining samples γ -activities induced by 14 MeV neutrons. Nuclear Instruments and Methods. 1994;B93: 464-468
- [14] Berrada M, Misdaq MA, Thallouarn P. Determination of potassium in beet by 14 MeV neutron activation analysis. Journal of Radioanalytical Chemistry. 1979;54:361
- [15] Brodsky A. Handbook of Radiation Measurement and Protection. Section A. Vol. 1. West Palm Beach, FL: CRC Press; 1978
- [16] Heitler W. The Quantum Theory of Radiation. 3rd ed. London: Oxford University Press; 1954
- [17] Gotoh H. Calculation of the self-absorption of gamma rays in a disc shaped source. Nuclear Instruments and Methods. 1973;107:199
- [18] Nelson WR, Hirayama H, Rogers DW. SLAC-report-265; December 1985